Available online at www.sciencedirect.com
SCIENCE DIRECT®

Journal of the European Ceramic Society 23 (2003) 3105–3112
www.elsevier.com/locate/jeurceramsoc

Mechanisms of crack propagation in dry plaster

Sylvain Meille[a,c], Malika Saâdaoui[b], Pascal Reynaud[a,*], Gilbert Fantozzi[a]

[a]*GEMPPM, INSA de Lyon UMR CNRS n° 5510 Villeurbanne, France*
[b]*LERSIM, EMI B.P. 765, Agdal Rabat, Morocco*
[c]*Lafarge LCR, B.P. 15, 38 291 St Quentin Fallavier Cédex, France*

Received 18 October 2002; received in revised form 23 January 2003; accepted 8 February 2003

Abstract

Controlled crack propagation tests were performed on single edge notched bend samples to investigate the crack growth behaviour of dry plaster. The influence of the relative notch depth on the crack resistance curve has been studied and appears to be very important. The results are discussed considering a qualitative model based on the specific microstructure of plaster and in situ observations of the crack propagation. Two mechanisms acting at different scales and undergoing complex interactions are involved: crack bridging by small gypsum crystals acting locally behind the crack tip and secondary cracking in a macroscopic frontal process zone. Interaction of the main crack with secondary ones undergoes substantial branching and crack accelerations leading to bridging destruction due to sudden crack opening.

Keywords: Crack growth; Plaster; *R*-curve

1. Introduction

Plaster, obtained by hydration of hemihydrate, $CaSO_4.1/2H_2O$, is known to be a porous brittle material, widely used in building applications. Dry plaster is characterised by a linear elastic macroscopic behaviour and it has been reported that its hardness and elastic modulus decrease with increasing porosity.[1,2] Under constant loading, it undergoes permanent deformation[3] that can be accentuated by moisture.

Due to its easy shaping, dry plaster can be used as a model material to study the mechanical behaviour of porous brittle solids, but only few works have been published on its fracture behaviour.[4–6] Veikinis et al.[4] have studied the initiation and propagation of cracks from holes in plaster samples subjected to compressive loading and have reported a discontinuous collapse process of the holes by the fracture of segments within areas of high stress concentration. Coquard et al.[5,6] have shown that the mechanical behaviour of dry plaster can be described by a Weibull's theory with a modulus less than 10. They reported that the plaster toughness is size dependent and have proposed a thermodynamic approach to its fracture.

Recently, a toughness value of 0.12 $MPa.m^{1/2}$ was measured in 3 point bending for a plaster with a water to gypsum ratio of 0.8, but higher value was obtained with the double torsion method.[7] The difference was attributed to the rising *R* curve behaviour observed in plaster as the double torsion values were obtained after a large amount of crack extension (typically 15 mm) and correspond to the plateau of the *R* curve. The same study revealed that during static loading, slow crack growth started from stress intensity factor values as low as 30% of the toughness. This was attributed to the linkage of the main propagating crack with secondary cracks in the frontal zone, occurring even at very low level stress.

The aim of this study is to investigate crack propagation mechanisms in plaster using the concept of the *R*-curve or K_R-curve (crack growth resistance versus crack extension). A rising *R*-curve is a consequence of energy dissipating mechanisms that occur ahead of the crack tip or at its wake region and reduce the stress intensity factor at the crack tip (crack shielding). If the reinforcing mechanisms extend over large crack extension, the *R* curve is both specimen geometry and size dependent.[8,9]

* Corresponding author.
E-mail address: pascal.renaud@insa-lyon.fr (P. Reynaud).

0955-2219/03/$ - see front matter © 2003 Elsevier Ltd. All rights reserved.
doi:10.1016/S0955-2219(03)00094-3

Although the R curve is not unique, it provides a more satisfactory description of the fracture behaviour than a unique parameter (K_{Ic} or G_{Ic}) as it involves both crack initiation and propagation. Moreover, R curve measurements coupled with the re-notching technique[10,11] that removes crack face interactions enable to evaluate the contribution of crack wake bridging, and that of crack tip mechanisms due to fracture process zone (FPZ). This technique based on compliance measurement after re-notching was first used in alumina[10] and adapted to estimate the FPZ size of mortar and cementitious pastes.[12]

2. Materials and experimental procedure

The material used in this study is plaster (gypsum $CaSO_4$,2 H_2O), prepared by hydration of β hemihydrate powder ($CaSO_4$,0.5 H_2O) with a water to plaster ratio of 0.8. The final porosity was about 55% and the density close to 1 g cm^{-3}. Rectangular bars with dimension $180\times40\times20$ mm^3 were molded by casting of plaster paste with a setting time of approximately 40 min.

Fig. 1 shows micrographs of a polished section and a typical fracture surface of plaster. It is to note the local heterogeneity of the microstructure, the principal aspect of which is the entanglement of needle shaped gypsum crystals about with 20 μm in length, and 2 μm in lateral dimension. The porosity consists of small, interconnected pores with approximately 1 μm size and large spherical pores (> 50 μm) formed by trapped air in the hemihydrate powder.

Crack propagation experiments were performed using a three-point bending fixture with a span of 140 mm on an Instron universal testing machine. Notches with a ratio of notch length to specimen width, α, in the range 0.3–0.75 were introduced in the centre of the samples by saw cutting. The load-point displacement was monitored with a linear variable differential transducer (LVDT) and the displacement rate was typically 5 μm mn^{-1}. The crack propagation was in situ monitored by a video-camera which allowed to point out some crack path characteristics especially from the observation of the open regions of cracks. However, optical measurement of the crack length was not possible due to the low contrast around the crack tip. But according to the linear behaviour of plaster and its low R curve effect,[7] the crack length was estimated with the compliance method, the accuracy of which will be discussed later, using the iterative relation of Tada:[13]

$$a_n = a_{n-1} + \frac{W - a_{n-1}}{2}\frac{C_n - C_{n-1}}{C_n} \quad (1)$$

where C_n and a_n are respectively the compliance and associated crack length values and W is the width of the specimen.

The crack growth resistance, K_R, was given by the applied stress intensity factor determined from the stable fracture load-displacement curve and the standard expression using the geometrical factor Y of Srawley:[14]

$$K_R = \frac{3}{2}\cdot\frac{PL}{BW^2}\cdot\sqrt{a}.Y \quad (2a)$$

$$Y(\alpha) = \frac{1.99 - \alpha(1-\alpha)\left(2.15 - 3.93\alpha + 2.7\alpha^2\right)}{(1+2\alpha)(1-\alpha)^{3/2}} \quad (2b)$$

with

P: applied load
a: crack length
L: span
W: width of the specimen
B: thickness of the specimen
α: relative notch depth ($=a/W$)

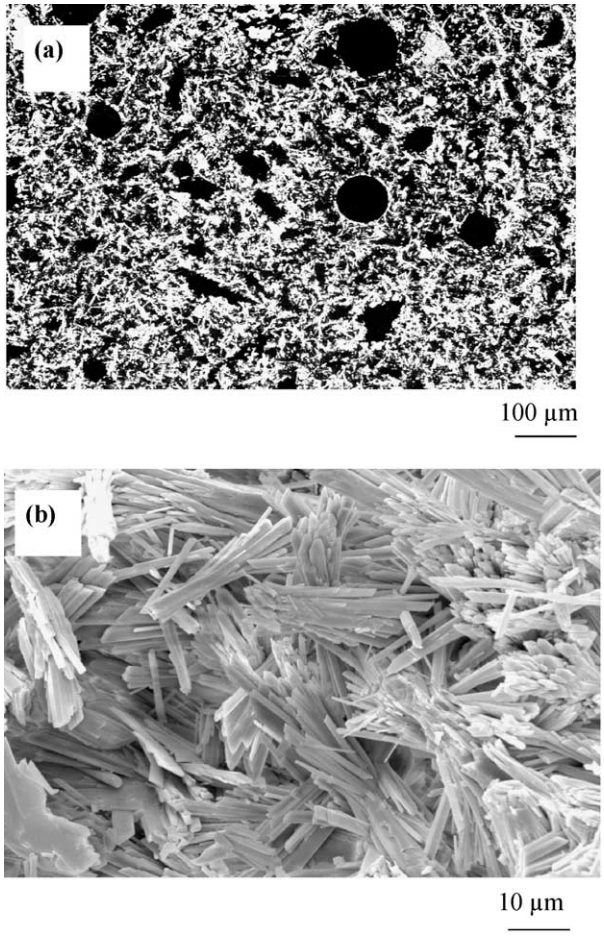

Fig. 1. SEM micrographs of (a) polished section, with pores in black and (b) fracture surface of plaster.

3. Experimental results

3.1. Load–displacement curves

The load–displacement curves obtained under the same loading conditions for different values of the relative notch depth, α, are shown in Fig. 2. A linear behaviour was first observed, followed by a deviation from linearity before the maximum load. Load drops (marked by an arrow in the figure) are often observed at the beginning of the non linear stage, and it could be associated to the onset of crack propagation. For all tests, the crack propagation globally occurred in a controlled manner, but load drops at a constant displacement were often observed in the decreasing part of the loading curve . In situ observation showed that the load drops are associated with accelerations of the main propagating crack due to the linkage with secondary cracks[7] and large air bubbles[15] present in the samples (Fig. 3) and corresponding to critical defects inducing plaster fracture.[16] Indeed, those load drops are less frequent and tend to disappear as the amount of the air bubbles decreases as it can be seen (Fig. 4) for a plaster grade having a more homogeneous repartition of pores compared to that used in the present work (Fig. 1a).

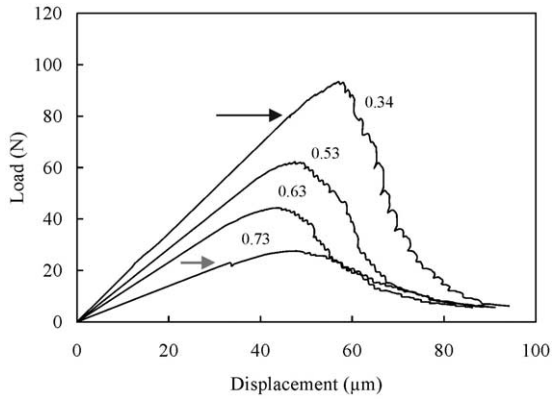

Fig. 2. Load–displacement curves for different notch depths. The arrows indicates the onset of crack propagation from the initial notch.

Fig. 3. Micrograph of fracture surface showing large air bubbles, potential sites of secondary cracking (sample thickness is 20 mm).

3.2. K_R-curves

The crack resistance curves obtained from the loading curves in Fig. 2 are shown in Fig. 5. Typical increase in the stress intensity factor, K_R, is first observed followed by a plateau region. The stress intensity factor at crack initiation K_0 is nearly constant, whereas a significant

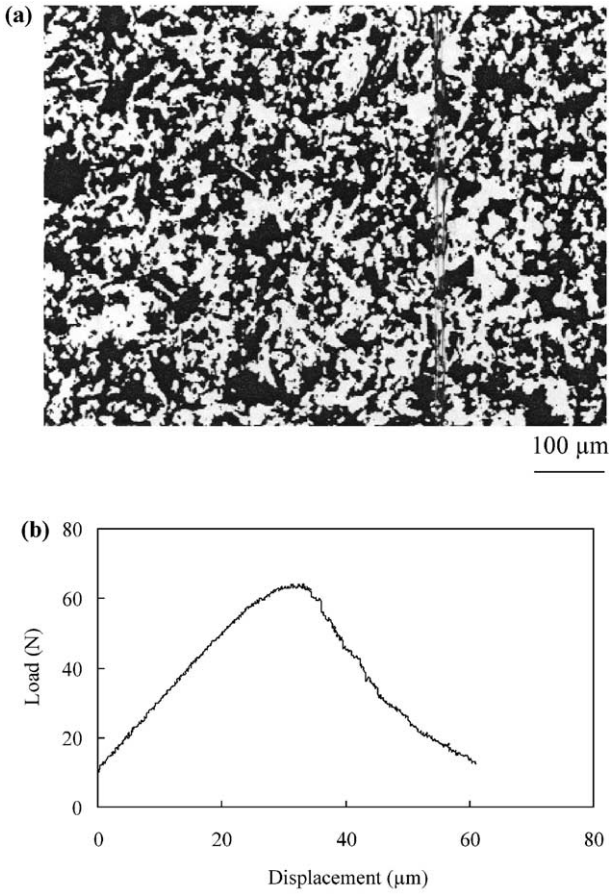

Fig. 4. Micrograph of polished section of an homogeneous grade plaster (a) and corresponding load-displacement curve (b) showing less load drops compared to that observed in the presence of air voids much more larger than the other pores (Figs. 1a and 2).

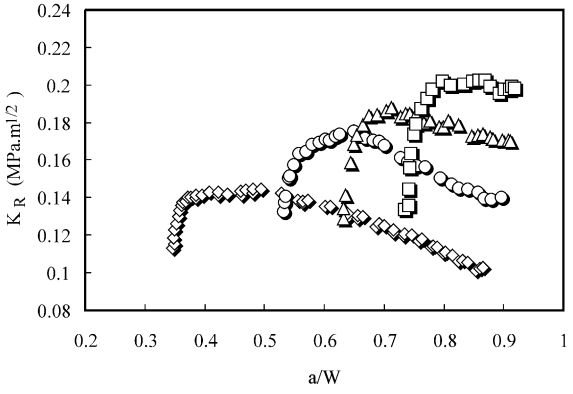

Fig. 5. Influence of the relative notch depth, $\alpha = a/w$, on the K_R-curves. (◇: $a/w = 0.34$, ○: $a/w = 0.53$, △: $a/w = 0.63$, □: 0.73).

increase of the plateau value, K_{max}, is noticed as the relative notch depth increases (Table 1).

The decrease observed in the K_R curves can be attributed to an underestimation of the length of large cracks by the compliance method. However, it has been shown[17] that this method gives results in a good agreement with those corresponding to measured crack lengths in the first stage of the crack propagation which will be considered in the following discussion.

3.3. Crack propagation

In situ observation revealed that the main crack propagation is initiated from the tip of the notch and is accompanied by a substantial secondary cracking, within a large damaged process zone, the size of which could reach several millimetres. This behaviour, that has already been observed in a similar plaster[7] is analogous to that generally observed in cementitious materials, specially mortar and concrete characterised by a large fracture process zone.[12] Some observed crack-path features are shown schematically in Fig. 6. The crack propagation occurs in a discontinuous manner by coalescence of the primary crack with secondary growing ones (Fig. 6a and b), inducing a sudden crack acceleration, correlated to the load drops during monotonic loading. Connection with non coplanar cracks induces substantial crack branching examples of which are shown in micrographs of Fig. 7. The main crack branches into two cracks, both of them growing simultaneously. Then, one of the cracks continues to propagate whereas the other arrests, often after undergoing a new branching. The arrested cracks tend to be closed, and become not visible when they are transferred to the wake of the main crack (dashed lines, Fig. 6b and c).

SEM observation of the damaged zone near the fracture surface of a broken sample revealed the existence of bridging by gypsum crystals in secondary cracks that remain open after testing (Fig. 8). Bridging is expected to be also active at the wake of the main crack as the gypsum crystals have the same role as in the secondary cracks. However, optical observation was difficult to achieve due to the presence of debris and to the closure of the bridged zone just behind the main crack tip.

Table 1
Iinfluence of the relative notch depth on K_0 and K_{max}

α = a/w	K_0 (MPa m$^{1/2}$)	K_{max} (MPa m$^{1/2}$)
0.34	0.11	0.145
0.53	0.13	0.17
0.63	0.125	0.185
0.73	0.13	0.2

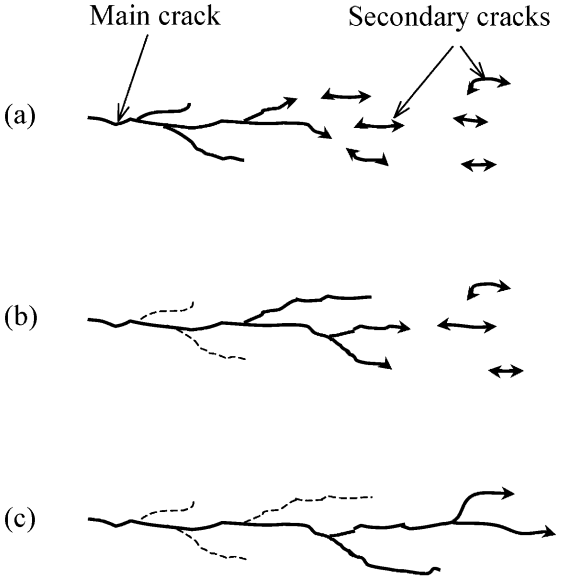

Fig. 6. Schematic illustration of the crack propagation process showing connection with secondary cracks (a–b) and branching.

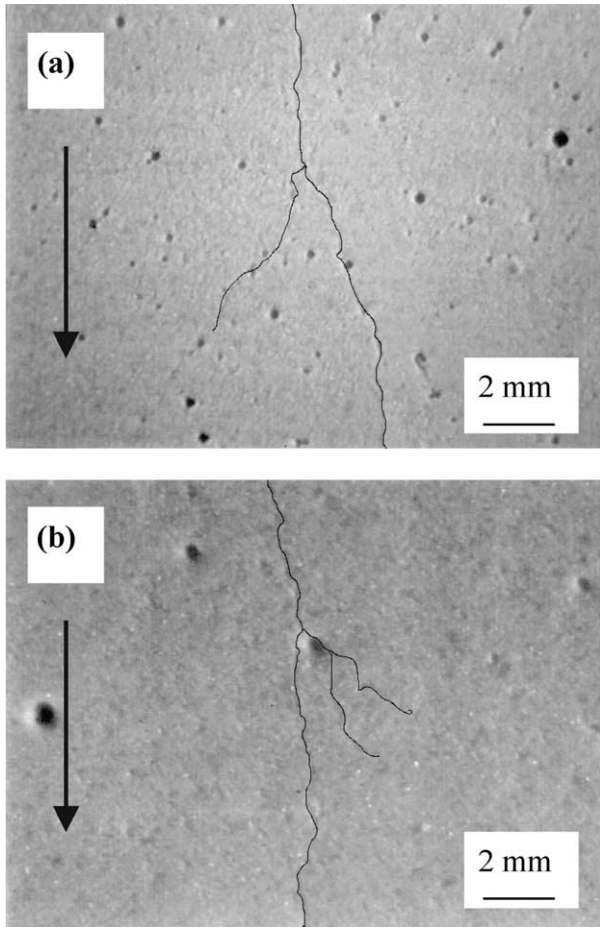

Fig. 7. Examples of micrographs of crack branching (for clarity, the crack path has been underlined). The arrows indicate the direction of crack propagation.

4. Discussion

4.1. Origin of secondary cracking

Secondary cracking has already been observed in plaster even at very low applied stresses during static loading of large double torsion samples.[7] The cracks can easily nucleate from large pores due to the stress concentration induced by the main crack or by adjacent pores. Such stress concentrations have been confirmed by a numerical simulation using a special finite element code based on image analysis and taking into account the geometrical aspects of the microstructure.[18] A two dimensional model was used considering a polished section of plaster subjected to tensile loading (Fig. 9a). The corresponding stress field resulting from the computation (Fig. 9b) shows a complex distribution with local stress concentrations (in red), within narrow bands representing potential sites for secondary crack nucleation and propagation.

Moreover, observation of fracture surfaces of plaster (Fig. 1b) does not show any broken gypsum crystals. Crack propagation occurs essentially by pull-out of gypsum crystals[15] according to their low bond energy. Local weak interfaces are thus also sites for crack nucleation. The presence of these weak regions is in agreement with the measurement of the contact forces between individual gypsum crystals by atomic force microscopy[19] that revealed a variation of the contact forces which may have low values depending on the orientation of gypsum crystals.

4.2. Crack growth mechanisms and qualitative modelling

For homogeneous dense materials exhibiting bridging, the bridged zone reaches a maximum size for a certain value of the crack opening displacement and thereafter, it translates with the crack tip for further crack propagation. This saturation corresponds to the plateau of the R curve which is not influenced by the size of the initial non-cracked ligament as it has been observed in alumina[20] where the rising R curve behaviour is only due to wake shielding by grain bridging. For plaster, the discontinuous aspect of the crack propagation suggests that the bridging by gypsum crystals cannot fully develop due to interactions with secondary cracking. Fig. 10 shows a simplified illustration of this interaction, which does not take into account crack branching and the evolution of secondary cracks. At the onset of crack propagation from the initial notch, contact shielding due to bridging by gypsum needles occurs behind the crack tip (Fig. 10a) and the bridged zone is expected to grow with the crack propagation (Fig. 10b). However, the distribution of the physical contacts is discontinuous according to the local heterogeneous repartition of pores in plaster. When the main crack links up with a secondary one or with a large pore, the crack opening displacement increases suddenly and that may lead to the destruction of the bridged zone (Fig. 10c). The process can start again at the new crack tip, with a different bridged zone both in size and in repartition of bridges, according to the heterogeneity of

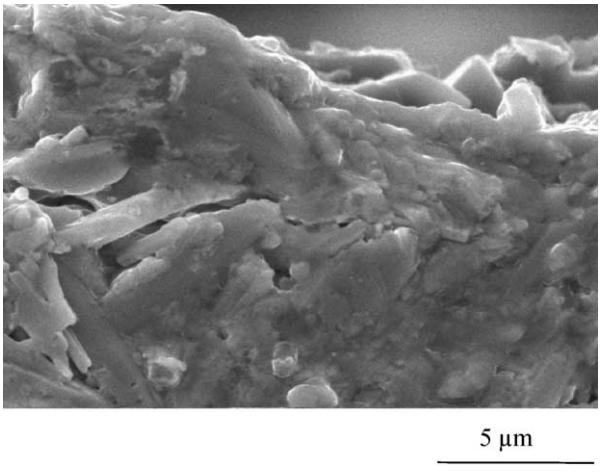

Fig. 8. Micrograph showing crack bridging by gypsum crystal.

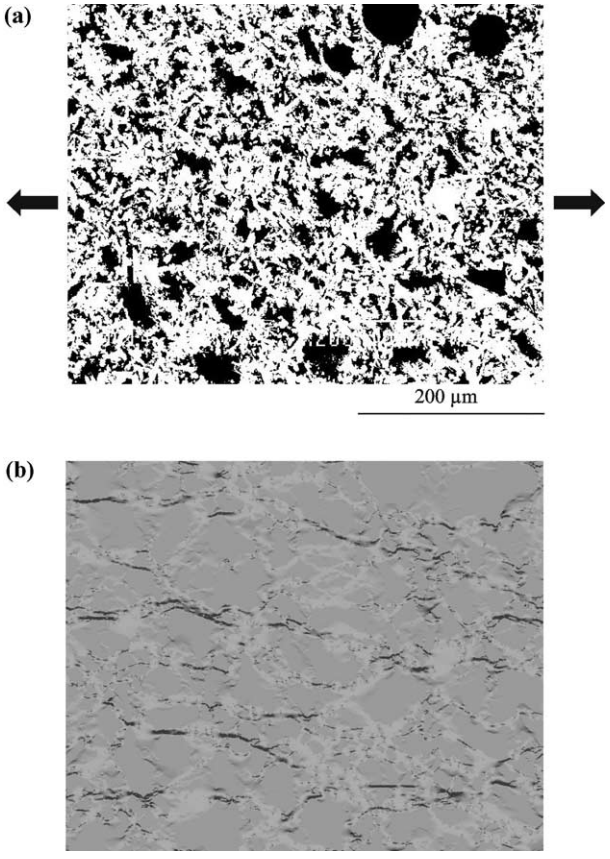

Fig. 9. Polished section of plaster subjected to an arbitrary tensile load in the direction indicated by the arrows (a) and the corresponding stress distribution (b) computed using a finite element code with image analysis. Colors correspond to different stress levels with maximum stress concentration (in red) favoring secondary cracking.

the microstructure (pores distribution and gypsum crystals orientation) and the secondary cracking. It leads to the appearances of drops on the curves of Fig. 5.

In fact, crack propagation in plaster must be considered as a three dimensional (3D) process due to the interaction with non planar secondary cracks and randomly distributed pores. As a consequence, the bridging zone may also be non planar, depending on the local crystals repartition and orientation. Such 3D character of crack propagation has already been pointed out in heterogeneous materials, particularly in concrete[21] in which high discontinuous macro-crack propagation has also been observed.

Mathematically, the crack tip shielding effects may be written in terms of a stress intensity balance, such that:

$$K_{tip} = K_{ap} - K_{br} - K_{cr} \quad (3)$$

where K_{tip} is the stress intensity factor at the crack tip, K_{ap} is the applied stress intensity factor, K_{br} and K_{cr} are respectively the contributions of bridging and secondary cracking. These two mechanisms act as shielding effects that decrease the stress intensity factor at the main crack tip. However, their contributions cannot be simply quantified due to their interaction, inducing a periodic reduction (or suppression) and reformation of the bridging zone when the main crack link up with secondary ones. The crack growth acceleration associated to this connection may be regarded as an anti-shielding effect that increases K_{tip}.

An attempt was made to distinguish the influence of the wake and the frontal mechanisms using the double notching method:[12] a sample with an extended crack of length, a, corresponding to the K_R-curve saturation, was re-notched by saw cutting to a distance about 5 mm behind the crack tip (Fig. 11). The K_R-curves determined before and after re-notching are shown in Fig. 12. K_R is substantially reduced after re-notching and remains constant for further crack propagation. Although the compliance method used for crack length evaluation does not allow determination of precise K_R values for large cracks, the decrease in K_R after re-notching even far from the crack tip indicates substantial wake effects that cannot only be attributed to bridging by gypsum crystals. The discontinuous character of the crack growth, and the substantial crack branching also, undergoes crack-surface interactions due to non-torn ligaments with larger size than those involved by needle bridging. Such behaviour has already been observed in cementitious materials with heterogeneous microstructure and weak zones leading to the formation of a fracture process zone.[12,22]

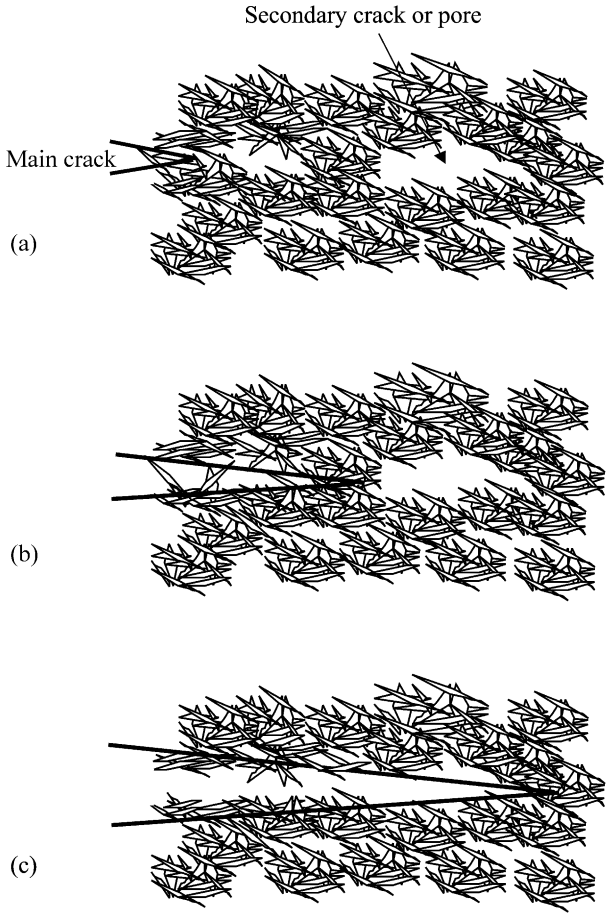

Fig. 10. Qualitative model of local crack bridging by gypsum needles illustrating bridging extension (a–b) and destruction by sudden crack opening due to connection with secondary cracks or large pores (c).

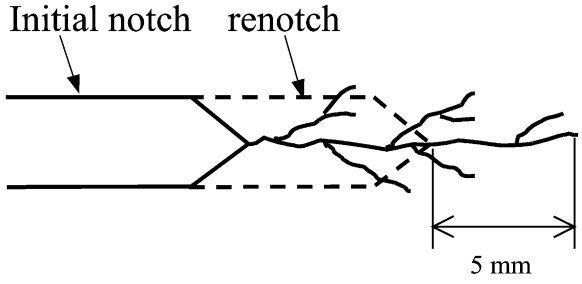

Fig. 11. Schematic illustration of the renotching procedure of a SENB sample.

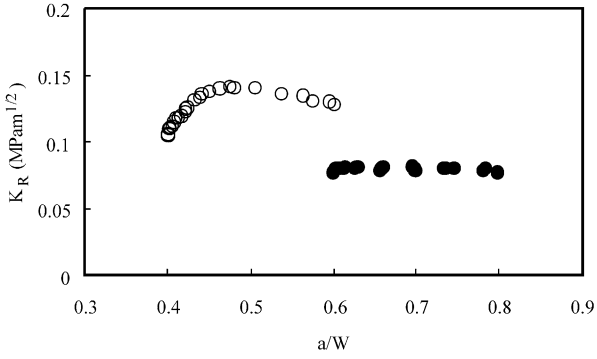

Fig. 12. Influence of renotching on the K_R-curve.

The different contributions are difficult to evaluate due to the complex crack growth process in plaster, but an equilibrium is reached between the shielding and the anti-shielding effects according to the observed plateau of the K_R curve, although it depends on the initial notch depth, the influence of which is discussed below. For cementitious materials,[12] it is now well admitted that the contribution to the reinforcement of the bridging by non-torn ligaments is much more important than that of local grain bridging by secondary phase, but further work is needed to establish such comparison in plaster.

4.3. Influence of the relative notch length on the K_R-curve

The influence of the relative notch depth on K_R-curves (Fig. 5) can be interpreted as a size effect, generally observed in brittle materials like cementitious materials[8,23] and ceramic composites:[24] the ligament, the larger the process zone and the higher the K_R plateau. However, in the case of plaster, the K_R plateau decreases with the ligament size, which can be attributed to a competition between the shielding and the anti-shielding mechanisms involved during crack propagation in plaster. This can be seen considering the stress distribution in the ligament of the tested samples, computed by finite element method at the onset of the crack propagation detected from the load displacement curves. The stress has the same tensile value $\sigma_0 = 2$ kPa at the notch tip and the size of the tensile zone, L_i, decreases with the notch depth (Fig. 13). Secondary crack nucleation and propagation can be active within the tensile zone even far from the notch tip as it may occur at very low tensile stresses.[7] As a consequence, the probability of crack connection, that reduces K_R by reduction of bridging effect, increases for large ligaments. This is in agreement with the decrease of the crack extension before the K_R plateau, Δa^*, as the ligament size increases (Table 2).

For precise interpretation of the size effect in plaster, further work is needed to quantify the contribution of the different crack growth mechanisms and their interaction; particularly, the bridging stress distribution and the process zone size have to be determined.

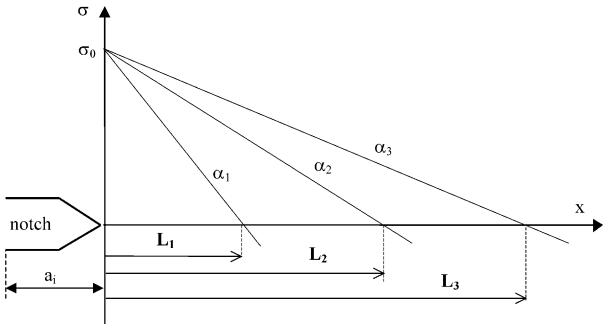

Fig. 13. Schematic illustration of the evolution of the tensile zone size, L_i with the relative notch depths, $\alpha_i = a_i/w$ ($\alpha_1 > \alpha_2 > \alpha_3$); x is the distance from the notch tip.

Table 2
Influence of the relative crack notch on the crack extension before the K_R-plateau

α	0.34	0.53	0.63	0.73
Δa^* (mm)	0.6	1.15	1.6	2.3

5. Conclusion

The results of the present study reveal for the first time the complex character of crack propagation in plaster due to its heterogeneous microstructure, consisting on an entanglement of elongated crystals and a bimodal distribution of pores with microscopic interconnected pores and large spherical air bubbles. It involves different mechanisms acting at different scales:

(1) Crack bridging by gypsum crystals, acting locally behind the crack tip.
(2) Secondary cracking operating in a macroscopic process zone around the crack tip.
(3) Substantial macroscopic crack branching that contribute to wake effects.

The material microstructure, especially the presence of large pores, and the low bond energy between crystals, allow nucleation and propagation of secondary cracks even far away from the main crack tip.

Crack bridging by gypsum crystals has been revealed by SEM observation. It operates simultaneously with secondary cracking leading to a complex interaction, a qualitative model of which has been proposed. It involves bridging degradation due to the sudden increase of the crack opening displacement induced by the linkage of the main crack with the secondary ones, or with large pores. The magnitude of such interaction depends on the stress field in the sample ligament, a large tensile zone favouring the initiation and propagation of cracks.

References

1. Soroka, I. and Sereda, P., Interrelation of hardness, modulus of elasticity and porosity in various gypsum systems. *J. Am. Ceram. Soc.*, 1968, **51**, 337–340.
2. Dalui, S., Roychowdhury, M. and Phani, K. K., Ultrasonic evaluation of gypsum plasters. *J. Mater. Sci.*, 1996, **31**, 1261–1263.
3. Sattler, H., Elastic and plastic deformations of plaster units under uniaxial compressive stress. *Materials and Structures*, 1974, **71**, 159–168.
4. Veikinis, G., Ashby, M. F. and Beaumont, P. W. R., Plaster of Paris as a model material for brittle porous solid. *J. Mater. Sci.*, 1993, **28**, 3221–3227.

5. Coquard, P., Boistelle, R., Amathieu, L. and Barriac, P., Hardness, elasticity modulus and flexion strength of dry set plaster. *J. Mater. Sci.*, 1994, **29**, 4611–4617.
6. Coquard, P. and Boistelle, R., Thermodynamical approach to brittle fracture of dry plaster. *J. Mater. Sci.*, 1996, **31**, 4573–4580.
7. Saâdaoui, M., Reynaud, P., Fantozzi, G., Péronnet, F. and Caspar, G. P., Slow crack growth study of plaster using the double torsion method. *Ceram. Int*, 2000, **26**, 435–439.
8. Cotterell, B. and Mai, Y. W., Crack growth resistance curve and size effect in the fracture of cementitious paste. *J. Mater. Sci.*, 1987, **22**, 2734–2738.
9. Lutz, E., Reichl, A. and Steinbrech, R., Size dependence of the *R*-curve of quasi-brittle materials, In *Fracture Mechanics of Ceramics,* Vol. **11**, ed. R.C. Bradt et al. New York, 1996, pp. 53–62.
10. Knehans, R. and Steinbrech, R., Memory effect of crack resistance during slow crack growth in notched alumina. *J. Mater. Sci. Lett.*, 1982, **1**, 327–329.
11. Lutz, E. H. and Sakai, M., R-curve and compliance change upon renotching. *J. Am. Ceram. Soc.*, 1993, **76**, 3113–3122.
12. Cotterell, B. and Mai, Y. W.. In *, Fracture Mechanics of Cementitious Materials*. Blackie Academic and Professional/Chapman and Hall, Glascow/London, 1996, pp. 294.
13. Tada, H., Paris, P. and Irwin, G., *The Stress Analysis of Cracks Handbook*. Del Research Corporation, 1973.
14. Srawley, J. E., Wide range stress intensity factor expressions of ASTM E 399 Standard fracture toughness specimens. *Int. J. Fract.*, 1976, **12**, 475–476.
15. Meille, S., *Etude du Comportement Mécanique du Plâtre Pris en Relation Avec sa Microstructure*, PhD thesis, INSA de Lyon, France, 2001.
16. Peronnet, F., *Comportement à la Rupture et Mécanismes de Propagation de Fissures dans les Plâtre Secs*. DEA report, INSA de Lyon, France, 1996.
17. Ebrahimi, M., Chevalier, J., Saâdaoui, M. and Fantozzi, G.Effect of the grain size on the crack propagation in alumina. In *Fracture Mechanics of Ceramics*, ed. R. C. Bradt, D. Munz, M. Sakai, V.Ya Shevchenko and K. W. White. Plenum Press, New York, 2002, pp. 273–286.
18. Meille, S. and Garboczi, E. J., Linear elastic properties of 2-D and 3-D models of porous materials made from elongated objects. *Mod. Simul. Mater. Sci. Eng.*, 2001, **9**, 371–390.
19. Finot, E., Lesniewska, E., Goudonnet, J. P. and Mutin, J. C., Correlation between surface forces and surface reactivity in the setting of plaster by atomic force microscopy. *Applied Surface Science*, 2000, **161**, 316–322.
20. Saâdaoui, M., Olagnon, C. and Fantozzi, G., Influence of precracking procedure, environment, temperature and microstructure on R-curve behaviour of alumina and PSZ ceramics. *J. Eur. Ceram. Soc.*, 1993, **12**, 361–368.
21. Van Mier, J., Mode I fracture of concrete: discontinuous crack growth and crack interface grain bridging. *Cem. Concr. Res.*, 1991, **21**, 1–15.
22. Schorn, H., Damage process and fracture mechanism of uniaxial loaded concrete. In *Micromechanics of Concrete and Cementitious Composites*, ed. C. Huet. Presses Polytechniques et Universitaires Romandes, Lausane, 1993, pp. 35–44.
23. Hu, X. Z. and Wittmann, F. H., An analytical method to determine the bridging stress transferred within the fracture process zone: II, Application to mortar. *Cem. Concr. Res.*, 1992, **22**, 559–570.
24. Conchin, F., *Comportement thermomécanique de composites 2D SiC/C/SiC*. PhD thesis, INSA de Lyon, France, 1994.